

Article

Modulating Biofunctional starPEG Heparin Hydrogels by Varying Size and Ratio of the Constituents

Petra Birgit Welzel [†], Silvana Prokoph [†], Andrea Zieris, Milauscha Grimmer, Stefan Zschoche, Uwe Freudenberg and Carsten Werner ^{*}

Leibniz Institute of Polymer Research Dresden (IPF), Max Bergmann Center of Biomaterials Dresden (MBC) & Technical University Dresden (TUD), Center for Regenerative Therapies Dresden, Hohe Strasse 6, 01069 Dresden, Germany; E-Mails: welzel@ipfdd.de (P.B.W.); prokoph@ipfdd.de (S.P.); zieris@ipfdd.de (A.Z.); grimmer@ipfdd.de (M.G.); zschoche@ipfdd.de (S.Z.); freudenberg@ipfdd.de (U.F.)

^{*} Author to whom correspondence should be addressed; E-Mail: werner@ipfdd.de; Tel.: +49-351-4658-531; Fax: +49-351-4658-533.

[†] Authors contributed equally.

Received: 3 December 2010; in revised form: 24 February 2011 / Accepted: 9 March 2011 /

Published: 14 March 2011

Abstract: Heparin and four-armed, end-functionalized polyethylene glycol (starPEG) were recently combined in sets of covalently linked biohybrid hydrogel networks capable of directing various therapeutically relevant cell types. To extend the variability and applicability of this novel biomaterials platform, the influence of size and molar ratio of the two building blocks on the hydrogel properties was investigated in the present study. Heparin and starPEG were converted in various molar ratios and in different molecular weights to tune swelling, stiffness and pore size of the obtained polymer networks. Hydrogels with a range of elastic moduli could be generated by controlling either the crosslinking density or the chain length of the starPEG, whereas altering the molecular mass of heparin did not significantly affect hydrogel strength. The concentration of heparin in the swollen gels was found to be nearly invariant at varying crosslinking degrees for any given set of building blocks but adjustable by the size of the building blocks. Since heparin is the base for all biofunctionalization schemes of the gels these findings lay the ground for an even more versatile customization of this powerful new class of biomaterials.

Keywords: heparin; star-shaped poly(ethylene glycol); hydrogel; network properties; molecular mass; biomimetic scaffold

1. Introduction

Hydrogels have been successfully used in biomedical fields due to their high water content, their advantageous mechanical properties and the weak non-specific interactions with molecular and cellular components of the biofluids [1-9]. The most recent and exciting applications of hydrogels are cell-based therapeutics [10-12] and soft tissue engineering [13-16]. To elicit desired cell response and coax cells to assemble into functional tissues, the materials that support and contact the cells need to be carefully designed (e.g., [17-19]). In various approaches it was shown that materials mimicking key parameters of the extracellular matrix (ECM) may directly affect cell growth and differentiation [20-23]. For hydrogels intended to trigger cellular fate decisions, critical design parameters include both biochemical properties and physical properties [18,19,24-28]. Thus, the elastic shear modulus of the fully swollen materials should be tunable in the range of 0.1 to 10 kPa to adjust the elasticity of soft tissues [26]. In addition, the hydrogel network should offer the possibility to incorporate appropriate bioactive moieties (e.g., cell binding domains, morphogens).

Motivated by the obvious need for cell-instructive biomaterials with tailor-made properties, we recently introduced a novel biohybrid hydrogel platform, which allows for decoupling of mechanical and biomolecular stimuli [29,30]. The gel system is a binary polymer network composed of star-shaped poly(ethylene glycol) (starPEG) and heparin, the latter being a base for a range of effective secondary biofunctionalization schemes. Attachment of adhesive ligands and loading of growth factors were found to be strictly correlated to the heparin concentration. This gel system offers most valuable options to explore the impact of different material properties on cell fate decisions, as, for example, shown for the stimulation of survival, proliferation and differentiation of neuronal and endothelial cells [29,31,32].

The aim of the present study was to further extend relevant properties of the novel materials by systematically changing the molar ratio and varying the molecular mass of the building blocks.

In the hybrid networks under consideration, the stiff, highly charged heparin molecule acts as multifunctional crosslinker [33] that provides the biological activity of the material. Its affinity to signaling molecules [34] allows, for example, the incorporation of growth factors into the meshwork by electrostatic interaction. The elasticity of the gel is provided by the flexibility of the synthetic starPEG molecule [33]. PEG is the most frequently used polyether in biomedical applications [9,35-37] and is known for its superior hydrophilicity and biocompatibility.

Three dimensional polymer networks were formed by chemical crosslinking of amino end-functionalized starPEG molecules ($M = 10,000$ or $19,000$ g/mol, respectively) with 1-ethyl-3-(3-dimethylaminopropyl) carbodiimide/*N*-hydroxysulfosuccinimid (EDC/sulfo-NHS) activated carboxylic acid groups of heparin ($M = 6,000$ or $14,000$ g/mol, respectively). Using three different combinations of these starPEG and heparin molecules, three different hydrogel series were prepared by mixing the building blocks in various molar ratios in each case. The physico-chemical properties of the different series were characterized by swelling experiments in phosphate buffered saline (PBS) and

oscillatory rheology. The mesh sizes of the polymer networks were approximated from the storage moduli of the swollen gels using the rubber elasticity theory [38]. The data were confirmed by studying the uptake behavior of fluorescence-labeled molecules of different size and shape into fluorescence-labeled hydrogels by confocal laser scanning microscopy (cLSM). Furthermore the chemical composition of the swollen scaffolds was calculated from the composition at preparation and volume change due to swelling.

With the reported approach a family of hybrid gels was obtained, each with constant amount of the bioactive component heparin and fine-tunable network properties, which permits the adjustment of important material properties to the requirements of various applications in tissue engineering.

2. Results and Discussion

2.1. Preparation of the starPEG Heparin Scaffolds

Heparin and starPEG molecules of various molecular masses (Figure 1(b)) were successfully crosslinked to form biohybrid hydrogels. The molar ratio of starPEG to heparin (γ) was varied from 1.5 to 6. As the general principle for gel formation, a defined number of the EDC/s-NHS activated carboxylic groups of the heparin were covalently crosslinked with terminating amino groups of starPEG (Figure 1(a)). Curing was finished at least after storage at room temperature overnight, as indicated by time dependent rheometry (see Supplementary Information). For example, the gels of the PEG10HEP14 series reached the gel point (point of crossover of G' and G'') after at least 2 hours (starPEG to heparin ratio of 1.5). Gels with higher starPEG to heparin ratio formed faster than those with lower ratios.

Figure 1. (a) Design of the starPEG heparin hydrogels. (b) Variation of heparin and starPEG building blocks.

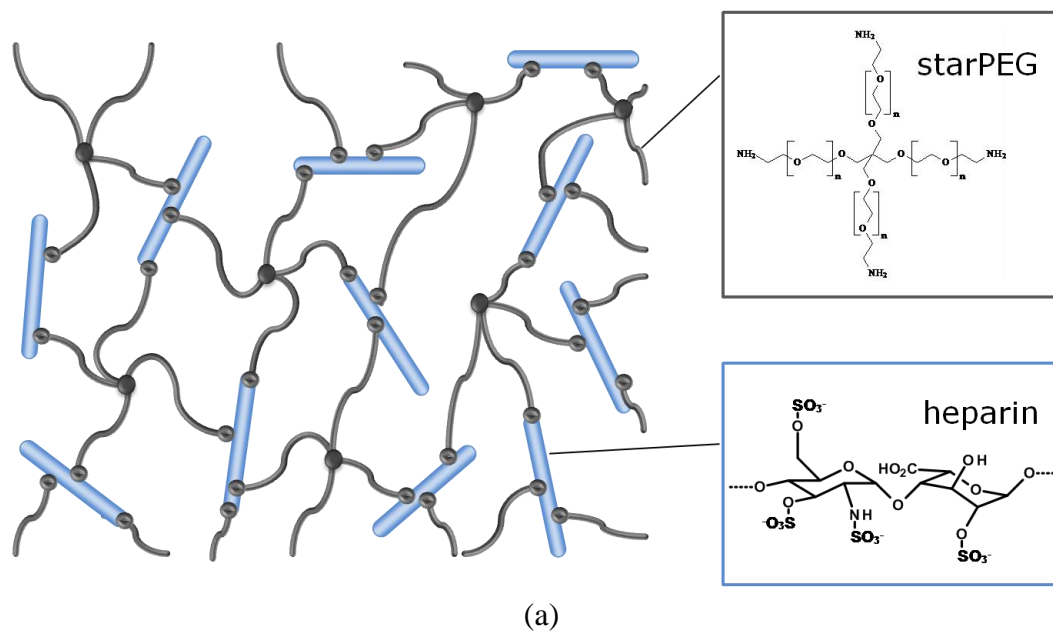
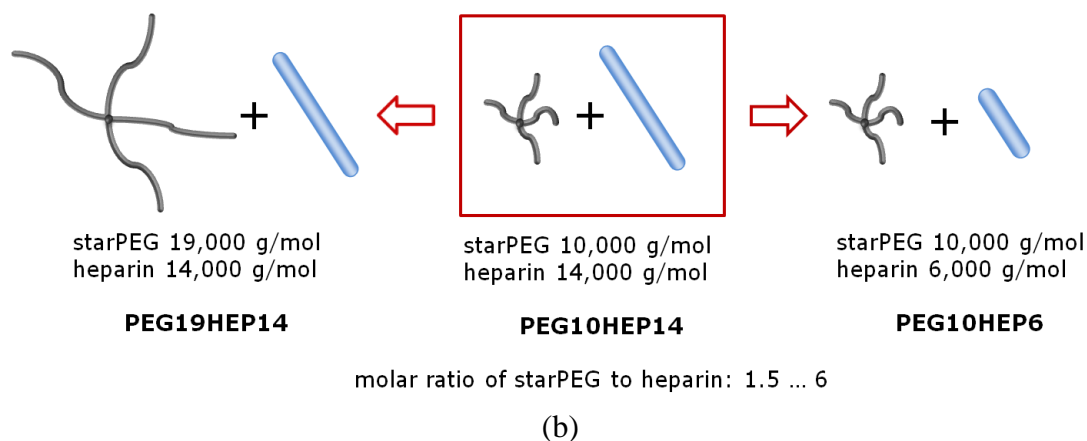


Figure 1. Cont.



Compared to previously reported biohybrid hydrogel systems [35,39-44] that used heparin as a pendant group our system is characterized by significantly higher heparin concentrations in the swollen matrices. Thus, the highly charged glycosaminoglycan heparin influences the network properties. Changing the relative heparin content in the reaction mixture changes both the crosslinking degree and the charge density within the gel and can consequently be used to tune elasticity and swelling. Thus, the heparin content of the swollen biomaterial can be controlled as discussed in the following sections.

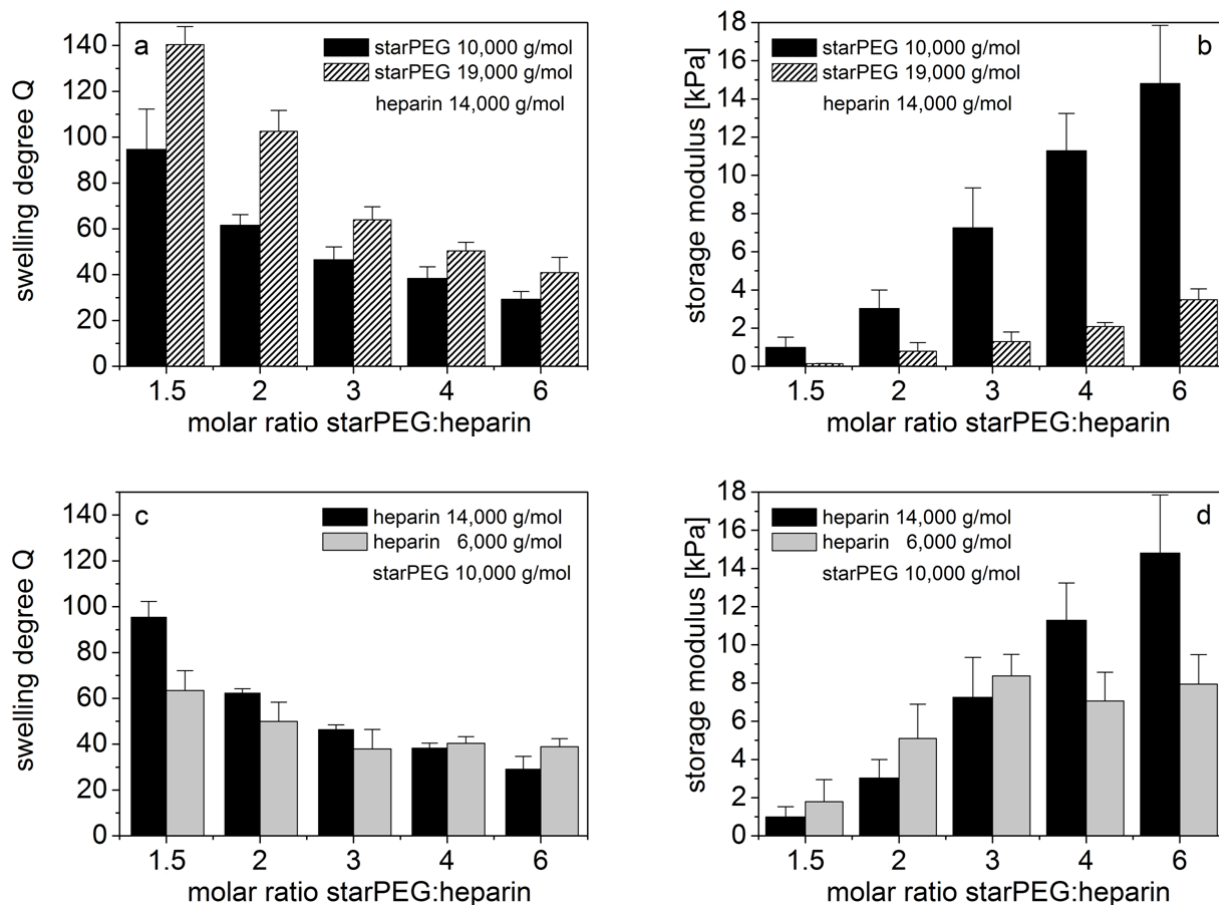
2.2. Gel Swelling in PBS and Viscoelastic Properties

After formation, the gels already consist of nearly 90% water, but are not completely saturated with water yet and swell or contract upon addition or evaporation of water. Since many favorable properties of hydrogels result from their hydrophilicity, the characterization of water-sorption is important and volumetric swelling ratios were measured as a means of determining the structural effects of varying starPEG and heparin molecular mass and starPEG to heparin molar ratios.

Furthermore, tunable mechanical properties of the swollen hydrogels are hypothesized to be an important characteristic in the design of a material implant. Therefore, these properties have been studied in the present work by oscillatory rheology. The frequency dependence of the storage and loss moduli was measured for PBS swollen hydrogels and the effects of molecular weight and ratio of the two building blocks were determined. For all gels the storage modulus G' is approximately two decades higher than the loss modulus G'' and independent of frequency for the measuring range of 0.1 to 10 rad/s (see Supplementary information). The loss modulus runs parallel to the storage modulus. These courses are characteristic for gels [45]. The phase angle, characterizing the ratio of the two moduli ($\tan \delta = G''/G'$) was always smaller than 3° . These data demonstrate that the starPEG heparin gels are almost ideal elastic materials in the frequency range studied, the viscous component can be neglected. The stability of the networks obtained through the covalent crosslinks is rather high.

By varying the molecular mass of starPEG and heparin or the starPEG to heparin ratio, gel properties can be controlled in a very broad range. Figure 2 illustrates the impact of composition of the hydrogel on swelling and mechanical properties.

Figure 2. (a) Swelling properties of starPEG-heparin hydrogels. The ratio of wet volume to dry volume is reported for PEG10HEP14 and PEG19HEP14 hydrogels relative to the molar starPEG to heparin ratio in the polymer network. (b) Comparison of storage moduli for swollen PEG10HEP14 and PEG19HEP14 hydrogels relative to the starPEG to heparin ratio in the polymer network. (c) Swelling properties of starPEG-heparin hydrogels. The ratio of wet volume to dry volume is reported for PEG10HEP14 and PEG10HEP6 hydrogels relative to the starPEG to heparin ratio in the polymer network. (d) Comparison of storage moduli for swollen PEG10HEP14 and PEG10HEP6 hydrogels relative to the starPEG to heparin ratio in the polymer network.



2.2.1. Influence of the starPEG to Heparin Molar Ratio

As illustrated in Figure 2(a,c), for given building blocks the increase of the starPEG to heparin molar ratio (γ) from 1.5 to 6 leads to a remarkable change in the hydration behavior. Increasing the starPEG to heparin ratio resulted in a decrease in volume swelling ratio Q in PBS. This effect was observed equally for gels containing low and high molecular mass starPEG, however it was more pronounced for the high molecular mass starPEG. In detail for PEG10HEP14 gels volume swelling ratio in PBS decreased from 95 ± 18 for a molar starPEG to heparin ratio of 1.5 to 29 ± 3 for a ratio of 6. For PEG19HEP14 gels it was reduced from 140 ± 8 for a molar ratio of 1.5 to 41 ± 7 for a ratio of 6.

Furthermore, with increasing starPEG to heparin ratios, similarly increasing storage moduli have been observed for all building block combinations investigated (Figure 2(b,d)). For example, for a 1.5 fold molar excess of starPEG storage modulus was $\sim 1,000$ Pa for hydrogels containing starPEG

$M = 10,000$ g/mol and heparin $M = 14,000$ g/mol whereas 6 fold excess led to storage moduli of about 15,000 Pa. In consequence, rising initial starPEG to heparin ratios lead to stiffer gels, while by decreasing the ratios softer gels are formed.

The different swelling behavior and storage moduli reflect the different crosslinking of the hydrogels [2,38] that is adjusted by the varying starPEG to heparin ratio. Heparin acts as a rigid multifunctional crosslinker for starPEG molecules. The higher the mol fraction of starPEG, the more end-monomers of different starPEG molecules will be covalently attached to the same crosslinker molecule. Thus, the effective functionality of the heparin molecules is determined by the molar ratio of the two building blocks before reaction. For given building blocks a higher mol fraction of starPEG leads to a stronger network with a higher number of functional crosslinks and a higher fraction of the elastic component. Highly crosslinked hydrogels have a tighter structure resulting in a higher storage modulus and less swelling compared to the hydrogels formed from building blocks of the same molecular mass but with lower crosslinking ratios. This holds true up to the maximal functionality, which equals the total number of carboxylic acid groups and thus correlates to the molecular mass of the heparin used (for heparin $M = 6,000$ g/mol only up to a molar ratio of 3, see below, Section 2.2.3). *Vice versa*, lowering the amount of starPEG results in more loosely crosslinked hydrogels, which can consequently take up more water and are softer.

For our system the influence of charged groups on equilibrium swelling additionally must be considered. The negative net charge of the hydrogels is rather high and dependent on the heparin concentration. Given this, the relative concentration of heparin in the cured reaction mixture should have a pronounced effect on the water uptake, and therefore volume increase of the hybrid hydrogels. In general, the water uptake is lower for gels prepared with a higher starPEG to heparin ratio. This can be attributed to not only the higher crosslinking degree, but also to the lower heparin concentration in the initial reaction mixture resulting in a lower charge density within the gel.

2.2.2. Influence of the starPEG Molecular Mass

Comparing hydrogels that contain 10,000 g/mol starPEG with those containing 19,000 g/mol starPEG, it can be noticed that increasing the molecular weight of starPEG at constant starPEG to heparin ratio leads to a significant increase in swelling and a complementary decrease in storage modulus (Figure 2(a,b)). This behavior results from the larger length of the arms of the used starPEG molecule that consequently leads to larger distances between two cross-linking points and therefore an increased ability to take up solvent and—keeping in mind that the starPEG is the flexible component—a higher flexibility at equal cross-linking degree compared to low molecular mass starPEG gels.

Changing the molecular mass of the building blocks also changes their relative volume fraction at a given molar starPEG to heparin ratio. The influence of the reduced relative volume fraction of heparin with increasing starPEG molecular mass, which should result in a decreased water uptake due to the reduced net charge of the network, is obviously smaller than the influence of PEG-arm length. In sum, swelling increases and the gels become softer.

2.2.3. Influence of the Heparin Molecular Mass

Figures 2(c,d) illustrate the impact of size of the heparin component on water uptake and storage modulus. Altering the molecular weight of the heparin crosslinker at constant starPEG to heparin ratio does not significantly influence the mechanical properties ($p > 0.05$). This may be due to the fact that the effective functionality of the heparin molecule only depends on the molar ratios of the two compounds and not on the maximal functionality of the heparin molecule itself that would be dependent on the number of disaccharide units per molecule (each disaccharide unit bears one reactive carboxylic acid group) and thus on the molecular mass.

The slightly lower swelling degrees for equally crosslinked heparin 6,000 g/mol gels compared to heparin 14,000 g/mol gels up to $\gamma = 3$ (significant for $\gamma = 1.5$ and 2) may be due to charge effects (osmotic pressure caused by trapped counterions). Decreasing the molecular mass of heparin results in a smaller volume fraction of the polyanionic gel component and consequently in a smaller negative net charge of the hydrogel. The lower amount of trapped counterions obviously results in a reduced water uptake. The differences in swelling could also be explained by a slightly lower molecular weight between crosslinks for the gels with the lower molecular mass heparin constituents.

The maximal functionality is about 28 for the 14,000 g/mol heparin and about 12 for the 6,000 g/mol heparin (assuming a molecular mass of approximately 500 g/mol per disaccharide unit). Thus, the maximal starPEG to heparin ratio possible for the high molecular weight heparin is higher ($\gamma = 7$) than for the low molecular weight heparin ($\gamma = 3$), if we assume that all four arms of the starPEG molecules are crosslinked. Above $\gamma = 3$ the number of crosslinks probably does not increase anymore and less than four arms of the starPEG molecules are bound to the 6,000 g/mol heparin, resulting in network defects. This maybe the reason for the nearly constant mechanical and swelling properties of PEG10HEP6 gels for $\gamma > 3$. Consequently, using high molecular weight heparin the storage modulus can be tuned over a wider range and stronger gels can be produced than with the low molecular weight heparin.

Heparin molecular weight also influences the number of free carboxylic acid groups available for secondary biofunctionalization at a given crosslinking degree, as will be discussed more in detail later (see Section 2.3. *Composition of the swollen hydrogel materials*).

In summary, based on the swelling and rheological experiments it was shown that the molecular weight of the starPEG component or the ratio of the building blocks in the initial reaction mixture extensively influence water uptake and storage modulus. This knowledge can finally be used to specifically tailor hydrogel properties. In this manner, using lower molar ratios of starPEG to heparin and/or using starPEG with higher molecular mass permits softer gels with higher swelling degrees to be produced. Thus, both softer, injectable gels and stiffer gels that may be used to generate polymer scaffolds of defined shape can be created based on the explored gel system.

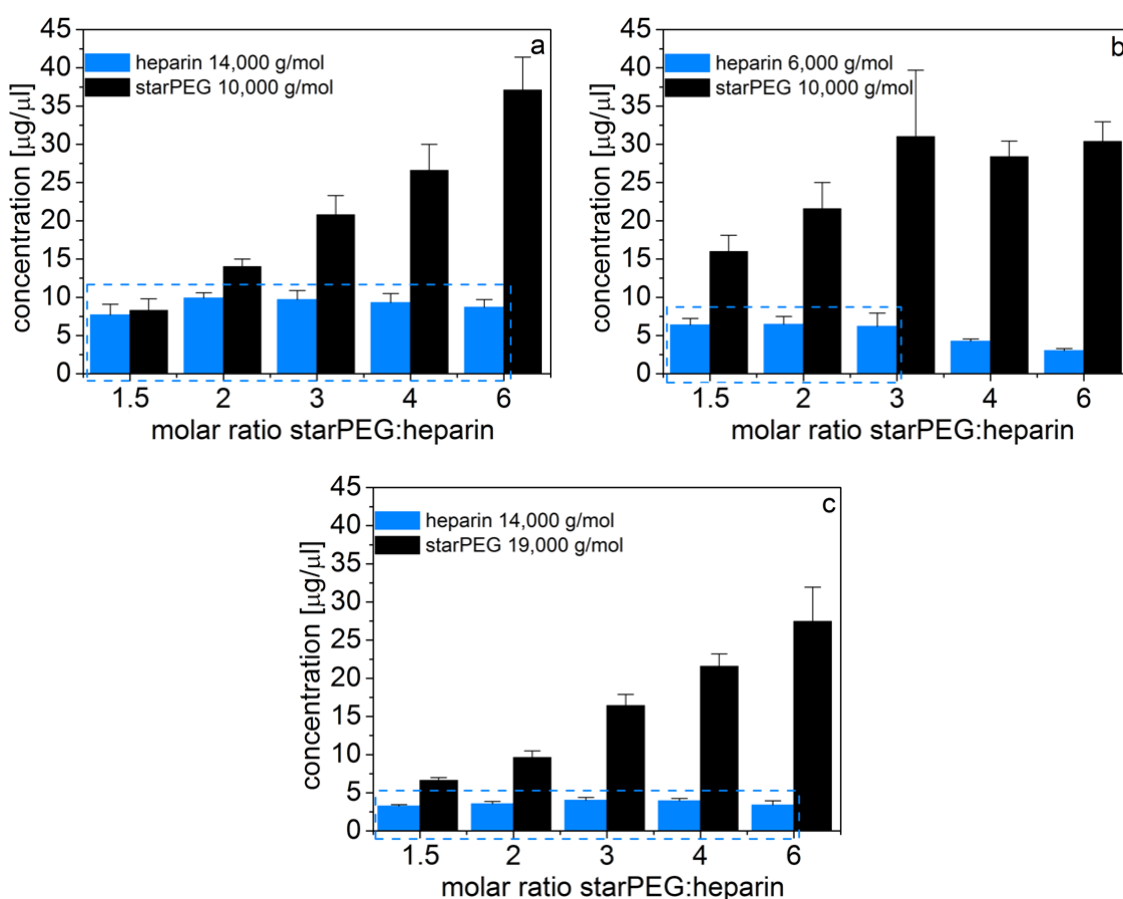
2.3. *Composition of the Swollen Hydrogel Materials*

Since we found that the swelling of the hydrogels depends on the crosslinking degree and the molecular mass of the building blocks, we next determined how this change in swelling affected the final composition of the PBS swollen hydrogels within the entire range of crosslinking degrees.

Therefore we normalized the heparin and starPEG amount in the reaction mixture to the volume of the swollen gel (calculated from volume swelling data).

Accordingly, we found that in PBS the initially different heparin concentrations are counterbalanced by a different swelling degree (*i.e.*, volume change) of the scaffolds. Thus, the heparin concentration in the final, swollen gels is constant for given building blocks and independent of the molar ratios of starPEG to heparin (Figure 3). For PEG10HEP14 gels a heparin content of approximately 9.1 ± 0.9 mg/mL was determined (Figure 3(a)).

Figure 3. Composition of the swollen starPEG-heparin hydrogels made from (a) 10,000 g/mol starPEG and 14,000 g/mol heparin, (b) 10,000 g/mol starPEG and 6,000 g/mol heparin, (c) 19,000 g/mol starPEG and 14,000 g/mol heparin relative to the starPEG to heparin ratio in the polymer network.



Furthermore, by utilizing different sizes of starPEG or heparin, the final heparin concentration in the scaffolds can further be varied. Specifically, using starPEG with $M = 19,000$ g/mol for gel formation instead of starPEG with $M = 10,000$ g/mol at invariant solid content (in the initial reaction mixture) leads to a reduction of the heparin concentration in the swollen gels by approximately 60% (3.6 ± 0.3 mg/mL, Figure 3(b)). By substitution of heparin $M = 14,000$ g/mol by heparin $M = 6,000$ g/mol a gel series with a constant heparin concentration of 6.4 ± 0.1 mg/mL is available for molar ratios between 1.5 and 3 ($\gamma = 3$ is the maximal starPEG to heparin ratio possible for the low molecular weight heparin, if we assume that all four arms of the starPEG molecules are crosslinked, see Section 2.2.3, Figure 3(c)).

Consequently, with this strategy, various gel series with constant heparin concentration each become available that can be fine-tuned in their physical network properties.

The starPEG content in the washed and swollen gels increased with rising molar ratios of starPEG and heparin in the reaction mixture irrespective of the starPEG and heparin molecular mass. This increase was moreover shown to reach a region of saturation at a final point when all carboxylic acid groups of heparin are cross-linked by the starPEG (e.g., for PEG10HEP6 above $\gamma = 3$). Furthermore, the starPEG content of the swollen hydrogel is directly correlated to the numbers of covalent bonds formed (*i.e.*, the crosslinking degree) and therefore to the storage modulus of the matrices, which is obvious from the comparison of storage modulus and starPEG concentration (see Figures 2 and 3). Again, this holds true for PEG10HEP6 gels at molar ratios over 3, where a further increase of starPEG in the initial reaction mixture does not increase the number of formed bonds and no increase in the starPEG concentration nor the storage modulus in the swollen gels is obtained (see Figure 2(d) and Figure 3(b)).

As heparin is the basis for the secondary biofunctionalization of the gels [29,32], these findings enable a versatile and independent adaptability of both mechanical and biomolecular parameters. One option consists of the reactive conversion of heparin with functional peptides such as cell adhesive ligands (RGD-peptides). Thus, by using gels of given starPEG and heparin species, *i.e.*, with constant heparin concentration, matrices with constant RGD concentration but varying crosslinking degree were obtained, as demonstrated in [29,32]. As another key advantage of the gel material, a wide variety of growth factors (such as basic fibroblast growth factor (FGF-2)) can be incorporated through noncovalent conjugation to heparin [29,32]. Consequently, structural and mechanical characteristics can be adapted independently of the biofunctionality of the scaffolds.

The reactive conversion of the non-crosslinked carboxylic acid groups of the heparin building blocks correlates with the total number of carboxylic acid groups per molecule (dependent on number of disaccharide units). Accordingly, for a given γ the number of free COOH groups is always larger for the high molecular weight heparin than for the low molecular weight heparin. Comparing the number of reactive groups for a starPEG to heparin ratio of 3, there are approximately 16 free COOH groups for the PEG10HEP14 gels whereas in the case of PEG10HEP6 gels there is no free COOH group left. Thus, variation of the heparin building block allows to further adjust the possibilities for covalent functionalization schemes of the resulting matrices.

2.4. Physical Network Structure—Mesh Size

Detailed knowledge about network parameters of the polymer hydrogels is of great importance. In this context, the mesh size of the network can be compared with the dimensions of molecules to be delivered. Theoretically, diffusion of solutes within the hydrogel matrix strictly requires mesh sizes larger than the hydrodynamic radii of the molecules to be delivered. Thus, the suitability of hydrogels as biomedical materials and their performance in a particular application depends to a large extent on their bulk structure. The hybrid hydrogels presented here consist of a dense network of macromolecular chains, which can neither be investigated by perfusion experiments nor visualized by microscopy. However, as revealed by rheology experiments, the examined hydrogels are supposed to show real elastic behavior, which enables the investigation of the network structure by means of the rubber elasticity theory (RET) [38]. As natural rubber, a hydrogel subjected to a relatively small deformation,

less than 20% (here: 3%), will fully recover to its original dimension in a rapid fashion [2,3]. RET allows an approximation of the molecular gel porosity. In this manner, it is possible to calculate the mesh size from the storage moduli of the swollen gels by Equation 2 (Experimental section) based on the affine network model [38].

With increasing starPEG to heparin ratio the mesh size of the network was found to be reduced (Table 1). This can be easily understood assuming that an increasing starPEG to heparin ratio in the initial reaction mixture leads to higher crosslinked gels and consequently the formed networks contain smaller pores. Besides this, the decreasing mesh size with increasing starPEG to heparin ratio was observed irrespective of the starPEG and heparin molecular mass. Nevertheless, as expected, at a given crosslinking degree, gels containing high molecular mass starPEG ($M = 19,000$ g/mol) had significantly larger pores compared to the starPEG ($M = 10,000$ g/mol) gels. The increased mesh size of high molecular mass starPEG thereby results from the larger chain length of the high molecular weight starPEG molecules. Consequently, after cross-linking of the elongated starPEG chains to heparin a larger distance between two adjacent cross-links is possible. As expected, changing the molecular mass of the heparin (crosslinker) does not influence the mesh size of the network significantly, as reflected already by the rheological experiments.

Table 1. Mesh size of various starPEG-heparin matrices calculated from the storage moduli of the swollen gels by Equation 2 (RET).

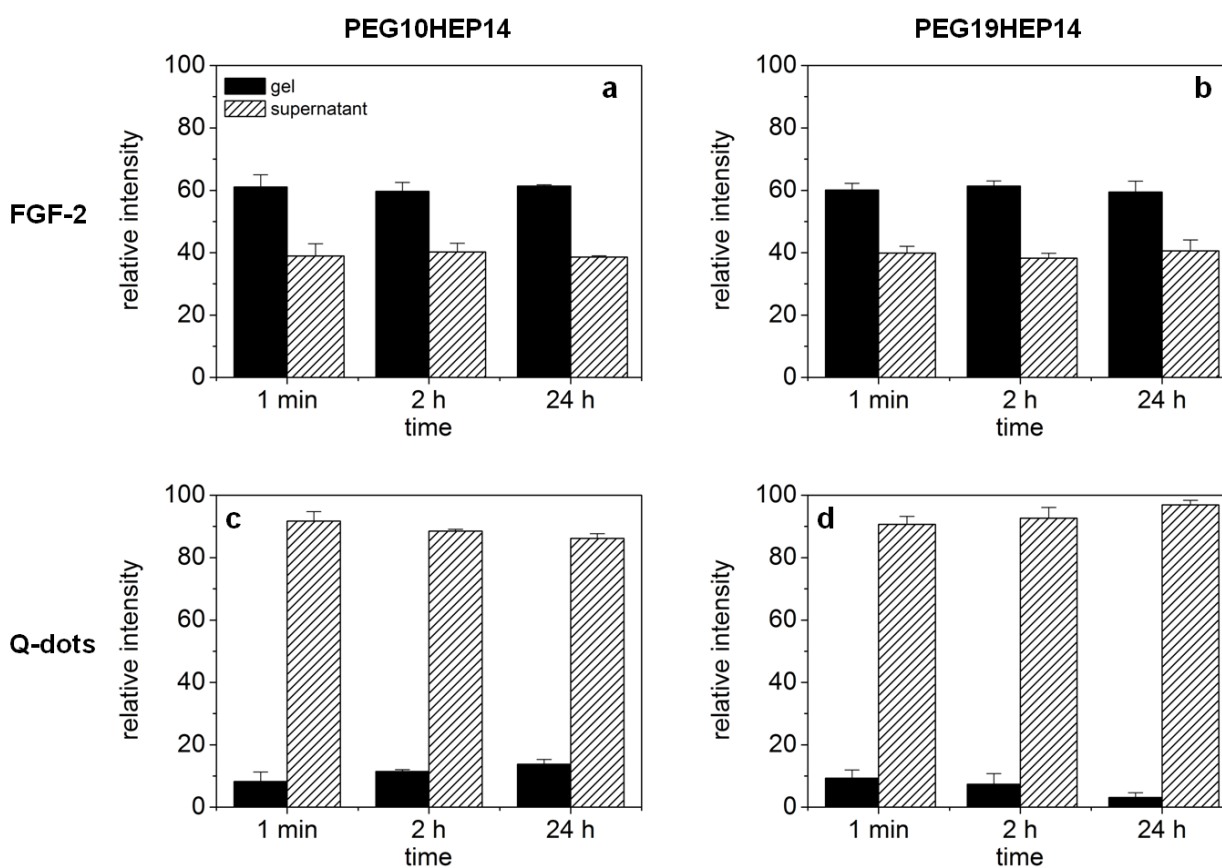
| molar ratio starPEG to heparin | pore size (RET) | | |
|-----------------------------------|-------------------|--------------------|--------------------|
| | PEG10HEP6 [nm] | PEG10HEP14 [nm] | PEG19HEP14 [nm] |
| 1.5 | 13 ± 3 | 16 ± 1 | 31 ± 1 |
| 2 | 9 ± 1 | 11 ± 2 | 17 ± 2 |
| 3 | 8 ± 1 | 8 ± 3 | 15 ± 2 |
| 4 | | 7 ± 3 | 13 ± 1 |
| 6 | | 6 ± 3 | 11 ± 1 |

In general mesh size is only a crude estimation of the average porosity in the synthetic network presuming ideal cross-linking. In reality, molecular defects such as unreacted groups leading to dangling chains and macroscopic inhomogenities will be present that substantially increase the effective mesh size. Physical entanglements, on the other hand, which are not accounted for in the estimation, will decrease the mesh size.

To unravel possible defects and inhomogenities the uptake of fluorescence-labeled molecules and quantum dots into the hydrogel networks was investigated by cLSM. Molecules/particles of different size were applied to starPEG heparin gels varying in molecular mass and molar ratio of their building blocks and consequently of different network structure. The uptake of fluorescence labeled FGF-2 into starPEG-heparin hydrogels is shown in Figure 4 (top). FGF-2, the smallest molecule used in cLSM uptake studies, is a round shaped molecule with a diameter of approx. 3×4 nm [46] and has a high affinity to heparin [34]. Comparing hydrogels containing building blocks of different molecular weight there was no significant difference concerning the uptake of FGF-2, as shown exemplarily for PEG10HEP14 and PEG19HEP14 hydrogels ($\gamma = 3$). The fact that FGF-2 penetrated all examined gel

matrices within seconds indicates that all gels have pores larger than the size of FGF-2. Irrespective of the gel type the FGF-2 intensity inside the gel is higher than in the supernatant already one minute after application (see Figure 4, top).

Figure 4. Average fluorescence intensity of TAMRA-labeled FGF-2 (top) and non targeted quantum dots (bottom) in supernatant (solution) and in the starPEG-heparin hydrogel body. Shown are mean values \pm SD for hydrogels with a starPEG to heparin ratio of 3 containing starPEG M = 10,000 g/mol (left) or starPEG M = 19,000 g/mol (right), respectively ($n = 2$, mean values represent average intensity over 3 z-lines in gel or supernatant). Measurements were performed by cLSM.



After penetration, FGF-2 showed a homogenous distribution throughout the entire gel, demonstrating the absence of any significant structural heterogeneities in the network and confirming the estimations of the RET that suggested the unrestricted penetration of FGF-2 even for gels with the highest degrees of crosslinking. The affinity of FGF-2 towards heparin does explain the observed accumulation of FGF-2 inside the gel body over time.

Figure 4 (bottom) illustrates the results of quantum dot (Q-dot) application onto the different starPEG-heparin hydrogels, again exemplarily shown for PEG10HEP14 and PEG19HEP14 hydrogels ($\gamma = 3$). The used non-targeted quantum dots (assumed to be not interacting with the polymer matrix) have a hydrodynamic diameter of approximately 45 nm according to the manufacturer's data sheet. Almost no fluorescence intensity was monitored inside the gel body after adding the quantum dots, independent of size and molar ratio of the building blocks and also of time. This indicates that the

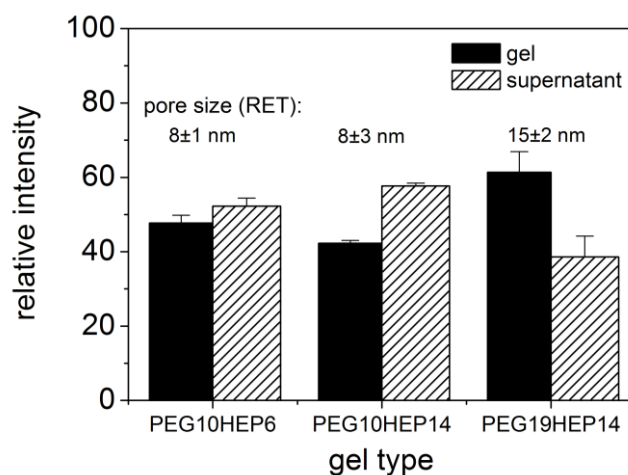
non-targeted quantum dots cannot penetrate the gel matrix and the mesh size of all examined gel types must be below the hydrodynamic diameter of 45 nm to hinder the uptake.

In summary the results of the uptake studies fit well to the mesh sizes calculated from mechanical properties, ranging from 6 to 31 nm, which is comparable to the porosity of many biological hydrogels [47,48] and allows for the unrestricted transport of nutrients, metabolism products, small-molecule drugs, and growth factors. However, the penetration of large biomacromolecules such as most matrix proteins (e.g., collagen, laminin, fibronectin) and glycosaminoglycans to the gels or the release of non-covalently entrapped entities can be sustained according to their hydrodynamic radii. When designed appropriately, the structure and mesh size of swollen hydrogels can be tailored to obtain desired rates of macromolecule diffusion utilizing the entrapment technique for such molecules [6]. Furthermore, unspecific accumulation of large macromolecules within the gel matrix could be efficiently prevented, by the mesh size and the protein-repellent character of the starPEG component.

After proving the upper size exclusion limit and confirming the accessibility for small molecules in a next step the “cut-off” region of the gels was evaluated in more detail. Therefore, the globular protein BSA was assumed to be a good probe with its slightly ellipsoid shape of $4 \times 4 \times 14$ nm [49,50], as it should show different penetration behavior related to the mesh sizes of the various gel types. These expected differences were confirmed by the uptake experiments, as exemplarily shown in Figure 5 for gels with a molar ratio of 3 containing different building blocks. Comparison of the results obtained for starPEG10HEP14 gels with those containing other building blocks (PEG19HEP14 and PEG10HEP6) for a given γ ($\gamma = 3$) confirms the good agreement with the mesh sizes determined by rheometry.

In addition, the accumulation of BSA at the gel boundary and inside the gel indicates that BSA seems to interact with the hybrid gel, leading to a higher overall intensity in the gel body. This might be caused by the affinity of BSA to many different ligand structures [51] and previously reported BSA-heparin interactions [52,53]. The described BSA accumulation within the gel matrix was qualitatively similarly observed for the other examined gel types, but with significant different time dependencies.

Figure 5. Average fluorescence intensity of TRITC-labeled BSA after 24 h in supernatant (solution) and in the starPEG-heparin hydrogel body. Shown are mean values \pm SD for different gel types with a starPEG to heparin ratio of 3 ($n = 2$, mean values represent average intensity over 3 z-lines in gel or supernatant). Measurements were performed by using cLSM. Comparison with the pore sizes determined from the storage moduli by using RET.



In summary, cLSM studies impressively confirmed the rheometry based mesh sizes of the matrices pointing furthermore to the fact that the hydrogels exhibit an almost “ideal” network structure showing few defects or heterogeneities.

3. Experimental Section

3.1. Materials

Porcine intestinal heparin sodium salt ($M = 14,000$ g/mol) was obtained from Calbiochem (Merck), Darmstadt, Germany ($M = 14,000$ g/mol) and from Dongying Tiandong Biochemical Industry Co. Ltd., China ($M = 6,000$ g/mol; Dalteparin). Amine end-functionalized 4-arm starPEGs ($M = 10,000$ and $19,000$ g/mol) were purchased from Polymer Source, Inc., Dorval, Canada. EDC and sulfo-NHS were obtained from Sigma-Aldrich, München, Germany. Deionized water was used in all experiments (MilliQ). PBS was obtained from Sigma, München, Germany. All of the chemicals were used as received.

3.2. Preparation of starPEG Heparin Gels

Gel formation occurred via crosslinking of amino end-functionalized starPEG with EDC/s-NHS-activated carboxylic acid groups of heparin. The molar ratio of the two macromers was varied while keeping the total solid content in the reaction mixture constant. StarPEG and heparin molecules with two different molecular weights were used in this study.

Heparin and starPEG were each dissolved in one-third of the total volume of deionized, decarbonized water (MilliQ) on ice. The components were individually dissolved in an ultrasonic bath filled with ice-cooled water for approximately 3–5 minutes, and afterwards all solutions were kept on ice. Applying the same procedure, EDC and s-NHS (molar ratio of EDC:sulfo-NHS of 2:1) were each dissolved in a sixth part of the total volume of ice-cold MilliQ. Based on the amount of NH_2 -groups of starPEG a twofold molar excess of EDC was used. Subsequently, EDC and s-NHS solutions were added to heparin, mixed well, and incubated for 15 minutes on ice to activate the heparin carboxylic groups. After that, the starPEG solution was added to the activated heparin and mixed for 15 seconds on a vortexer (at 900 rpm, Thermomixer Comfort, Eppendorf, Hamburg, Germany). The molar ratios of starPEG to heparin used in these studies were 6, 4, 3, 2, and 1.5). The reaction mixtures were allowed to cure at room temperature overnight. All hydrogels were formed with a constant total macromer (starPEG and heparin) concentration of 11.5 to 11.7% (w/w) in water. Consequently the heparin and starPEG contents in the reaction mixtures gels varied from gel to gel.

For preparation of free-floating gel disks, 67 μL of the liquid gel mixture were placed onto a hydrophobic glass cover slip of 9 mm diameter and covered with a second hydrophobic one. Both cover slips have been treated with hexamethyldisilazane (Fluka) from vapor phase. After polymerization over night at 22 $^\circ\text{C}$ in a humidified atmosphere, the cover slips were removed. For uptake studies of fluorescence labeled molecules surface bound gels with a final thickness of approx. 50 μm were prepared. These gels were labeled by mixing heparin with 5% of Alexa 488-labeled heparin. 3.5 μL of liquid gel solution have been pipetted onto a freshly APTES-amino functionalized glass-bottom 24-well plate (Greiner Bio-One GmbH, Frickenhausen,

Germany) to allow covalent attachment of heparin through its activated carboxylic acid groups [29]. In order to spread the solution equally, an ethylen-chlorotrifluorethylen-copolymer slide (Goodfellow, Cambridge, England) was placed onto the gel solution in the glass bottom wells. As previously described, the gel polymerized over night and after removal of the foil gels were washed in phosphate buffered saline (PBS, Sigma-Aldrich) to remove EDC/s-NHS and any non-bound starPEG/heparin.

3.3. Swelling Measurements

The initial diameters of the free standing disks (see preparation) were measured with digital vernier calipers. Swelling studies were carried out in PBS (pH 7.4) at room temperature. The hydrogel disks were immersed in a sufficient amount of the buffer and their diameters were measured with the vernier calipers over time. At each sampling time swelling medium was exchanged (every hour for four hours and once again after 24 hours). At least after 24 hours, equilibrium was reached. The final diameter of the swollen disks was measured. Experiments were carried out at least four times. The degree of volume swelling Q was calculated as follows:

$$Q = V/V_0 = (d/d_{\text{reac}})^3 \cdot V_{\text{reac}}/V_0$$

$$V_0 = n_{\text{PEG}} \cdot v_{\text{PEG}} + n_{\text{HEP}} \cdot v_{\text{HEP}} \quad (1)$$

where d is the diameter of the swollen gel disk, d_{reac} the diameter of the unswollen gel disk (cured reaction mixture), V_{reac} the volume of the cured reaction mixture and V_0 the volume of the dry gel. The molar volumes of the heparin ($v_{\text{HEP}} (M = 6,000 \text{ g/mol}) = 3,038 \text{ cm}^3/\text{mol}$, $v_{\text{HEP}} (M = 14,000 \text{ g/mol}) = 7,089 \text{ cm}^3/\text{mol}$) and the starPEG species ($v_{\text{PEG}} (M = 10,000 \text{ g/mol}) = 8,006 \text{ cm}^3/\text{mol}$, $v_{\text{PEG}} (M = 19,000 \text{ g/mol}) = 15,728 \text{ cm}^3/\text{mol}$) were calculated from the densities, which were determined by means of helium pycnometry (Ultrapycnometer 1000T, Quantachrome Instruments, USA).

3.4. Calculation of Heparin and starPEG Content in the PBS Swollen Scaffolds

The starPEG and heparin contents in the swollen gels were calculated from the heparin and starPEG content in the reaction mixtures and the volume swelling data.

3.5. Rheological Measurements for Mechanical Characterization of the PBS Swollen Hydrogels

Storage and loss moduli of the swollen gels (PBS) were obtained by performing oscillatory shear experiments on an ARES LN2 rotational rheometer (TA Instruments, Eschborn, Germany). A parallel plate geometry was used for these measurements (plate diameter 25 mm, gap width in the range of 1.2 to 1.5 mm). Disks of starPEG-heparin gels were prepared and swollen in PBS as described above (3.3. Swelling measurements). Frequency sweeps were performed at 25 °C with a strain amplitude of 3% over a frequency range of 10^{+2} – $10^{-1} \text{ rad s}^{-1}$. Both storage and loss modulus, respectively, were measured as a function of the shear frequency in a minimum of 3 independent measurements (each with three samples). Mean values of the storage and loss modulus of a frequency range of 10^{+1} – $10^{-1} \text{ rad s}^{-1}$ were calculated.

3.6. Calculation of Average Mesh Size

The average mesh size (distance between two entanglement points) ξ was calculated from the storage modulus G' based on RET [38] using the following equation:

$$\xi = \left(\frac{G' N_A}{RT} \right)^{-1/3} \quad (2)$$

where G' is the storage modulus, N_A the Avogadro constant, R the molar gas constant, and T the temperature.

3.7. Uptake of Molecules Monitored by Confocal Laser Scanning Microscopy (cLSM)

Besides rheometry, cLSM was used as another method to estimate the mesh size of the different hydrogels types. For this, the uptake of fluorescence labeled molecules or particles of various sizes into fluorescence labeled hydrogels has been studied.

While BSA-tetramethylrhodamine isothiocyanate (TRITC) was commercially available (Molecular Probes, USA), Fibroblast Growth Factor (FGF-2, Miltenyi, Germany) had to be labeled using FluoReporter® Tetramethylrhodamine (TAMRA) Protein Labeling Kit according to the manufacturer's instructions (Molecular Probes, distributed by Invitrogen, Netherlands).

The quantification of molecule-uptake into the hydrogels was performed with Leica SP5 confocal laser scanning microscope (pinhole of the aperture 53.1 μm). In general, fluorescence labeled molecules and the quantum dots were excited with a DPSS laser at 561 nm (laser intensity 20%) and their emission has been monitored in the range of 570–630 nm. The fluorescence intensity of Alexa 488-labeled hydrogels has been quantified after excitation with an argon laser (excitation wavelength 488 nm, laser intensity 20%). The emission of Alexa 488 was hereby measured in the range of 500–550 nm.

For time-dependent uptake studies, PBS on top of the gels has been exchanged against 5 $\mu\text{g/mL}$ TAMRA-FGF-2, 5 $\mu\text{g/mL}$ TRITC-BSA or 2 μM quantum dots (Q-Tracker 655, Invitrogen), respectively. Pictures were taken with a 40 \times oil immersion objective (HCxPL APO, Leica) at sequential scanning mode in xz-direction 1 min, 2 h and 24 h after addition of the molecules. For quantification of the fluorescence intensity the average over three z-lines for each gel in the supernatant and in the gel body has been determined. Relative intensities of fluorescence were calculated as percentage of the overall intensity, whereas the total intensity is the sum of the intensity in the gel and the intensity in the supernatant.

3.9. Data Analysis

All data collected are presented as mean \pm standard deviation of three or more samples. Statistical analysis was performed by one-way analysis of variance (ANOVA) and post-hoc Turkey-Kramer multiple comparison test. P values less than 0.05 were considered statistically significant.

4. Conclusions

Tissue engineering strategies require biomaterials with bioactivity and mechanical properties both being variable and independently adjustable over a wide range. To address this aim the network design

of a recently developed modular starPEG heparin hydrogel system was extended by varying size and ratio of the two building blocks. Heparin and starPEG molecules of varied molecular mass were crosslinked covalently to form biohybrid hydrogels of varying properties. The elasticity, pore size and the swelling of the gels could be modulated by the ratio of the two building blocks and by the molecular weight of the starPEG macromer, whereas the molecular weight of the heparin crosslinker hardly affected gel stiffness. Swelling slightly decreased with decreasing molecular weight of heparin. These trends in network characteristics were explained by the properties of the different building blocks (chain length, number of charged groups, number of functional groups).

A key feature of the modular hydrogel system is the constant heparin concentration of the swollen gels at varying physical network properties for given building blocks. This was found for all starPEG/heparin combinations used in this study, independent of their molecular mass. The constant heparin concentration of the gels permits a uniform secondary biofunctionalization of gel materials with different physical properties. By using starPEG or heparin of different molecular weight, the heparin concentration in the swollen gels can be modulated, too. Thus, heparin-starPEG hydrogels allow for the independent tuning of biomolecular functionalization and physical characteristics across a wide range of relevant parameters.

In summary, binary biohybrid hydrogels with tailor-made mechanical properties and biomolecular composition can be customized to support a range of tissue engineering schemes. As structural and biomolecular properties of the networks can be modulated independent from each other over a wide range, the system offers valuable options to dissect different microenvironmental signals acting on cells *in vitro* and *in vivo*.

Acknowledgements

We thank Lisa Naujox, Claudia Renneberg and Ron Dockhorn for performing part of the swelling and rheological experiments, Konrad Schneider for density measurements of starPEG and heparin and Mikhail Tsurkan for fluorescence labeling of heparin (all Leibniz Institute of Polymer Research Dresden).

U.F. and C.W. were supported by the Deutsche Forschungsgemeinschaft through grants WE 2539-7/1 and FOR/EXC999, and by the Leibniz Association. S.P. and C.W. were supported by the Seventh Framework Programme of the European Union through the Integrated Project ANGIOSCAFF. A.Z. was supported by the Dresden International Graduate School for Biomedicine and Bioengineering.

References

1. Hubbell, J.A. Hydrogel systems for barriers and local drug delivery in the control of wound healing. *J. Control. Release* **1996**, *39*, 305-313.
2. Peppas, N.A. Hydrogels in pharmaceutical formulations. *Eur. J. Pharmacol.* **2000**, *50*, 27-46.
3. Peppas, N.A.; Hilt, Z.; Khademhosseini, A.; Langer, R. Hydrogels in biology and medicine: From molecular principles to bionanotechnology. *Adv. Mater.* **2006**, *18*, 1345-1360.

4. Elisseeff, J.H.; Yamada, Y.; Langer, R. Biomaterials for tissue engineering. In *Tissue Engineering and Biodegradable Equivalents: Scientific and Clinical Applications*; Lewandrowski, K.-U., Wise, D.L., Yaszemski, M.J., Gresser, J.D., Trantolo, D.J., Altobelli, D.E., Eds.; Marcel Dekker, Inc.: New York, NY, USA, 2002; pp. 1-23.
5. Hoffman, A.S. Hydrogels for biomedical applications. *Adv. Drug Deliv. Rev.* **2002**, *43*, 3-12.
6. Lin, C.C.; Metters, A.T. Hydrogels in controlled release formulation: Network design and mathematical modeling. *Adv. Drug Deliv. Rev.* **2006**, *58*, 1379-1408.
7. Ulijn, R.V.; Bibi, N.; Jayawarna, V.; Thornton, P.D.; Todd, S.J.; Mart, R.J.; Smith, A.M.; Gough, J.E. Bioresponsive hydrogels. *Mater. Today* **2007**, *10*, 40-48.
8. Lutolf, M.P. Spotlight on hydrogels. *Nat. Mater.* **2009**, *8*, 451-453.
9. Zhu, J. Bioactive modification of poly(ethylene glycol) hydrogels for tissue engineering. *Biomaterials* **2010**, *31*, 4639-4656.
10. Jen, A.C.; Wake, M.C.; Mikos, A.G. Review: Hydrogels for cell immobilization. *Biotechnol. Bioeng.* **1996**, *50*, 357-364.
11. Lysaght, M.J.; Aebischer, P. Encapsulated cells as therapy. *Sci. Am.* **1999**, *280*, 76-82.
12. Tibbitt, M.W.; Anseth, K.S. Hydrogels as extracellular matrix mimics for 3D cell culture. *Biotechnol. Bioeng.* **2009**, *103*, 655-663.
13. Lee, K.Y.; Mooney, D.J. Hydrogels for tissue engineering. *Chem. Rev.* **2001**, *101*, 1869-1879.
14. Varghese, S.; Elisseeff, J.H. Hydrogels for musculoskeletal tissue engineering. *Adv. Polym. Sci.* **2006**, *203*, 95-144.
15. Hahn, M.S.; McHale, M.K.; Wang, E.; Schmedlen, R.H. West, J.L. Physiologic pulsatile flow bioreactor conditioning of poly(ethylene glycol)-based tissue engineered vascular grafts. *Ann. Biomed. Eng.* **2007**, *35*, 190-200.
16. Lin, C.C.; Anseth, K.S. PEG Hydrogels for the controlled release of biomolecules in regenerative medicine. *Pharm. Res.* **2008**, *26*, 631-643.
17. Lauffenburger, D.A.; Griffith, L.G. Who's got pull around here? Cell organization in development and tissue engineering. *Proc. Natl. Acad. Sci. USA* **2001**, *98*, 4282-4284.
18. Drury, J.L.; Mooney, D.J. Hydrogels for tissue engineering: Scaffold design variables and applications. *Biomaterials* **2003**, *24*, 4337-4351.
19. Brandl, F.; Sommer, F.; Goepferich, A. Rational design of hydrogels for tissue engineering: Impact of physical factors on cell behavior. *Biomaterials* **2007**, *28*, 134-146.
20. Balgude, A.P.; Yu, W.; Szymanski, A; Bellamkonda, R.V. Agarose gel stiffness determines rate of DRG neurite extension in 3D cultures. *Biomaterials* **2001**, *22*, 1077-31084.
21. Levental, I.; Georges, P.C.; Janmey, P.A. Soft biological materials and their impact on cell function. *Soft Matter* **2007**, *3*, 299-306.
22. Leach, J.B.; Brown, X.Q.; Jacot, J.G.; DiMilla, P.A.; Wong, J.Y. Neurite outgrowth and branching of PC12 cells on very soft substrates sharply decreases below a threshold of substrate rigidity. *J. Neural. Eng.* **2007**, *4*, 26-34.
23. Discher, D.E.; Janmey, P.; Wang, Y.L. Tissue cells feel and respond to the stiffness of their substrate. *Science* **2005**, *310*, 1139-1143.
24. Schwarz, U.S.; Bischofs, I.B. Physical determinants of cell organization in soft media. *Med. Eng. Phys.* **2005**, *27*, 763-772.

25. Wong, J.Y.; Leach, J.B.; Brown, X.Q. Balance of chemistry, topography and mechanics at the cell-biomaterial interface: Issues and challenges for assessing the role of substrate mechanics on cell response. *Surf. Sci.* **2004**, *570*, 119-133.
26. Engler, A.J.; Sen, S.; Sweeney, H.L.; Discher, D.E. Matrix elasticity directs stem cell lineage specification. *Cell* **2006**, *126*, 677-689.
27. Straley, K.S.; Heilshorn, S.C. Independent tuning of multiple biomaterial properties using protein engineering. *Soft Matter* **2009**, *5*, 114-124.
28. Yeung, T.; Georges, P.C.; Flanagan, L.A., Marg, B.; Ortiz, M.; Funaki, M.; Zahir, N.; Ming, W.; Weaver, V.; Janmey, P.A. Effects of substrate stiffness on cell morphology, cytoskeletal structure, and adhesion. *Cell Motil. Cytoskeleton* **2005**, *60*, 24-34.
29. Freudenberg, U.; Hermann, A.; Welzel, P.B.; Stirl, K.; Schwarz, S.C.; Grimmer, M.; Zieris, A.; Panyanuwat, W.; Zschoche, S.; Meinhold, D.; Storch, A.; Werner, C. A starPEG-heparin hydrogel platform to aid cell replacement therapies for neurodegenerative diseases. *Biomaterials* **2009**, *30*, 5049-5060.
30. Tsurkan, M.V.; Chwalek, K.; Levental, K.R.; Freudenberg, U.; Werner, C. Modular starPEG-heparin gels with biofunctional peptide linkers. *Macromol. Rapid Commun.* **2010**, *31*, 1529-1533.
31. Zieris, A.; Prokoph, S.; Welzel, P.B.; Grimmer, M.; Levental, K.R.; Panyanuwat, W.; Freudenberg, U.; Werner, C. Analytical approaches to uptake and release of hydrogel-associated FGF-2. *J. Mater. Sci. Mater. Med.* **2010**, *21*, 914-923.
32. Zieris, A.; Prokoph, S.; Levental, K.R.; Welzel, P.B.; Grimmer, M.; Freudenberg, U.; Werner, C. FGF-2 and VEGF functionalization of starPEG-heparin hydrogels to modulate biomolecular and physical cues of angiogenesis. *Biomaterials* **2010**, *31*, 7985-7994.
33. Sommer, J.-U.; Dockhorn, R.; Welzel, P.B.; Freudenberg, U.; Werner, C. Swelling Equilibrium of a binary polymer gel. *Macromolecules* **2011**, *44*, 981-986.
34. Capila, I.; Linhardt, R.J. Heparin-protein interactions. *Angew. Chemie Int. Ed.* **2002**, *41*, 390-412.
35. Benoit, D.S.; Anseth, K.S. Heparin functionalized PEG gels that modulate protein adsorption for hMSC adhesion and differentiation. *Acta Biomater.* **2005**, *1*, 461-470.
36. Lutolf, M.P.; Raeber, G.P.; Zisch, A.H.; Nicola, T.; Hubbell J.A. Cell-responsive synthetic hydrogels. *Adv. Mater.* **2003**, *15*, 888-892.
37. Raeber, G.P.; Lutolf, M.P.; Hubbell, J.A. Molecularly engineered PEG hydrogels: A novel model system for proteolytically mediated cell migration. *Biophys. J.* **2005**, *89*, 1374-1388.
38. Rubinstein, M.; Colby, R.H. *Polymer Physics*; Oxford University Press: Oxford, UK, 2003.
39. Seal, B.L.; Panitch, A. Physical polymer matrices based on affinity interactions between peptides and polysaccharides. *Biomacromolecules* **2003**, *4*, 1572-1582.
40. Cai, S.; Liu, Y.; Zheng Shu, X.; Prestwich, G.D. Injectable glycosaminoglycan hydrogels for controlled release of human basic fibroblast growth factor. *Biomaterials* **2005**, *26*, 6054-6067.
41. Tae, G.; Scatena, M.; Stayton, P.S.; Hoffman, A.S. PEG-crosslinked heparin is an affinity hydrogel for sustained release of vascular endothelial growth factor. *J. Biomater. Sci. Polym. Ed.* **2006**, *17*, 187-197.
42. Nie, T.; Akins, R. E., Jr.; Kiick, K.L. Production of heparin-containing hydrogels for modulating cell responses. *Acta Biomater.* **2009**, *5*, 865-875.

43. Jia, X.; Kiick, K.L. Hybrid multicomponent hydrogels for tissue engineering. *Macromol. Biosci.* **2009**, *9*, 140-156.
44. Benoit, D.S.; Durney, A.R.; Anseth, K.S. The effect of heparin-functionalized PEG hydrogels on three-dimensional human mesenchymal stem cell osteogenic differentiation. *Biomaterials* **2007**, *28*, 66-77.
45. Clark, A.H.; Ross-Murphy, S.B. Structural and mechanical properties of biopolymer gels. *Adv. Polym. Sci.* **1987**, *83*, 57-192.
46. Ago, H.; Kitagawa, Y.; Fujishima, A.; Matsuura, Y.; Katsube, Y. Crystal structure of basic fibroblast growth factor at 1.6 Å resolution. *J. Biochem.* **1991**, *110*, 360-363.
47. Mason, M.N.; Metters, A.T.; Bowman C.N.; Anseth K.S. Predicting controlled-release behavior of degradable PLA-b-PEG-b-PLA hydrogels. *Macromolecules* **2001**, *34*, 4630-4635.
48. Cruise, G.M.; Scharp, D.S.; Hubbel, J.A. Characterization of permeability and network structure of interfacially photopolymerized poly(ethylenglycol) diacrylate hydrogels. *Biomaterials* **1998**, *19*, 1287-1294.
49. Wright, A.K.; Thompson, M.R. Hydrodynamic structure of bovine serum albumin determined by transient electric birefringence. *Biophys. J.* **1975**, *15*, 137-141.
50. Bloomfield, V. The structure of bovine serum albumin at low pH. *Biochemistry* **1996**, *5*, 684-689.
51. Daughaday, W.H. Steroid protein interactions. *Physiol. Rev.* **1959**, *39*, 885-902.
52. Hattori, T.; Kimura, K.; Seyrek, E.; Dubin, P. Binding of bovine serum albumin to heparin determined by turbidimetric titration and frontal analysis continuous capillary electrophoresis. *Anal. Biochem.* **2001**, *295*, 158-167.
53. Wassell, D.T.H.; Embery, G. Adsorption of chondroitin-4-sulphate and heparin onto titanium: Effect of bovine serum albumin. *Biomaterials* **1997**, *18*, 1121-1126.